

Neutral gas temperature estimates in an inductively coupled CF₄ plasma by fitting diatomic emission spectra

Brett A Cruden,* M V V S Rao,* Surendra P Sharma and M Meyyappan

NASA Ames Research Center

Moffett Field, CA 94035

This work examines the accuracy of plasma neutral temperature estimates by fitting the rotational band envelope of different diatomic species in emission. Experiments are performed in an inductively coupled CF₄ plasma generated in a Gaseous Electronics Conference reference cell. Visible and ultraviolet emission spectra are collected at a power of 300 W (~ 0.7 W/cm²) and pressure of 30 mtorr. The emission bands of several molecules (CF, CN, C₂, CO and SiF) are fit simultaneously for rotational and vibrational temperatures and compared. Four different rotational temperatures are obtained: 1250 K for CF and CN, 1600 K for CO, 1800 K for C₂, and 2300 K for SiF. The vibrational temperatures obtained vary from 1750-5950 K, with the higher vibrational temperatures generally corresponding to the lower rotational temperatures. These results suggest that the different species have achieved different degrees of equilibration between the rotational and vibrational modes and may not be equilibrated with the translational temperatures. The different temperatures are also related to the likelihood that the species are produced by ion bombardment of the surface, with etch

* Eloret Corporation

products like SiF, CO and C₂ having higher temperatures than species expected to have formed in the gas phase.

I. Introduction

In a recent publication, we demonstrated the importance of neutral gas heating in reactor-scale simulations of plasma processing.¹ Given the effect neutral heating can have on the plasma, it is important to measure the neutral temperature in any comprehensive plasma study, though more often than not, this parameter is not measured. A number of different techniques have been used to estimate neutral temperatures in plasmas, including analysis of rotational and vibrational spectra in absorption,^{2,3} emission,⁴⁻⁷ or fluorescence,⁷ measurements of Doppler broadening in absorption^{8,9} or fluorescence,^{9,10} and measurements of species flux through an orifice.^{11,12} Of these techniques, Doppler broadening is the most robust way to directly measure the translational temperature of selected species, however to measure the Doppler linewidth, high resolution spectroscopic equipment is required. The measurement of species flux through an orifice can provide the neutral translational temperature near a surface and is fairly straightforward in an inert gas such as argon. However, application of this technique in reactive gases requires some assumptions regarding accurate neutral measurements, or constancy of pumping speeds. Two independent means of using this data to estimate temperature ^{have} yielded temperatures that differ by as much as 40%.¹² Any temperature measurement made by absorption spectroscopy will suffer from spatial averaging with cold gases outside of the plasma and may not be representative of the true

neutral temperature.¹³ Several assumptions are also involved in using the rotational temperature from emission as an estimate of translational temperature.

Estimates of neutral temperatures in plasmas have yielded a wide range of results. In our model of an inductively coupled CF_4 plasma in the GEC Cell at $\sim 1 \text{ W/cm}^3$, neutral temperatures in the range of 400-650 K were predicted.¹ Here, the heat resulted primarily from exothermic chemical reactions (charge exchange, dissociative recombination, ion-ion recombination) in the system. Using FTIR, we estimated neutral temperatures in the range of 300-500 K for the same system, though noted these temperatures were likely underestimates of the true temperature.¹³ Hebner reports temperatures of 550-1000 K in Ar plasmas at comparable power levels, determined from the linewidths of Ar in both absorption and fluorescence.⁹ He attributed the heating of argon ions to collisions in the presheath. It seems probable that the elevated neutral temperature is achieved through charge exchange with these ions. Singh, et. al., used a mass spectrometer sampling through an orifice in a homebuilt ICP to estimate neutral temperatures in the range of 450-930 K near the chamber wall in CF_4 at somewhat lower power densities.¹² Kiehlbach and Graves report modeling and experimental results ranging from 1200-2100 K, for 100-500 mtorr CF_4/O_2 at power densities of $0.5\text{-}2.0 \text{ W/cm}^3$.¹⁴ Their model showed that Franck-Condon and ion/neutral heating were the most important heating mechanisms. Donnelly and Malyshev estimated temperatures from 650-1250 K from analysis of N_2 emission spectra at 0.4 W/cm^3 for an inductively coupled Cl_2 discharge.¹⁵ In their work, heating was attributed primarily to the energy released by electron-impact dissociation. Temperatures reported in capacitive discharges typically range from 300-600 K.^{2,3,6-8}

The approach of using rotational emission spectra to estimate the translational temperature is fairly simple, as it requires only a spectrometer. It can be easily integrated into a commercial etcher, as it does not require complicated lasers and is non-intrusive, unlike typical mass spectrometer configurations. It is possible to perform the fit at low resolution, where the rotational peaks overlap and the band envelope, rather than individual peaks, can be fit. However, there are several potential problems with this approach. Foremost among these are assumptions of equilibration:

- 1) The rotational population of the species is thermally equilibrated
- 2) The rotational temperature is equilibrated with the translational temperature
- 3) The rotational temperature of the excited state responsible for emission is equilibrated with the ground state temperature.
- 4) The rotational temperature of one species in the discharge is equilibrated with that of other species in the discharge

To address the first assumption, it is necessary to individually measure each rotational line and fit their normalized intensities to a Boltzmann population. This has been done successfully in capacitively coupled plasmas,⁷ however we are not aware of this having been done in an inductively coupled plasma. The observation that the band envelope can be fit adequately¹⁵ may indicate that this assumption is at least reasonable. Even if assumption (1) is not exactly satisfied, it may be possible to measure an "effective" rotational temperature, as is often done with the electron temperature in non-Maxwellian plasmas. It seems unlikely that assumption (2) will be satisfied in this event, however. Assumption (2) can be verified by measuring the Doppler linewidth

simultaneously, though we are not aware of any studies of this nature. Assumption (3) is dependent on the lifetime of the excited state and the means of excitation and will be addressed in some detail here. Assumption (4) is addressed in this work by simultaneously estimating the rotational and vibrational temperatures of several different diatomic species.

II. Experimental

The experiments here were performed on an inductively coupled Gaseous Electronics Conference (GEC) Cell equipped with a spectrometer, as detailed in our previous work.^{16,17} The data reported here was collected at 300 W coil power in a 30 mtorr CF₄ plasma. The bulk of the plasma extends over a radius between 5-6 cm,¹⁸ and the separation between quartz coupling window and electrode is 3.2 cm, giving a plasma volume of ~300 cm³. The power coupling efficiency has been estimated at $73 \pm 2\%$ by a plasma impedance monitor (Scientific Systems), giving an estimated power density of 0.7 ± 0.2 W/cm³. The spectrometer and photodiode array give a data spacing of 0.23 Å/pixel and can simultaneously collect ~460 Å worth of the spectrum at a time. A series of spectra at wavelengths ranging from 1900 to 9500 Å are collected with ~1 min of integration time each. The more prominent emission bands that can be attributed to diatomic molecules are then analyzed for rotational temperature.

III. Theoretical

The theory behind fitting rotational spectra has been described in some detail by multiple authors.^{4,6} In this work, we have followed a similar procedure to that of previous work, though in some cases at a higher level of theory. The instrument line

shape was determined by fitting the empirical line shape of Refs. 4,6 to atomic lines observed in the spectrum, at similar wavelength ranges. To obtain the rotational fit, it is necessary to calculate both the energies of transition and the relative intensities of each line. As many of the spectra fit here involved radical species, it was often necessary to use a higher level of theory, accounting for spin-splitting of the spectra and satellite bands. In many of these cases, we have also considered the coupling of rotation and electronic motion, important when there is a net electronic spin or if one of the states has a non-zero orbital angular momentum (i.e. is not a $^1\Sigma$ state). The direct application of a Honl-London factor used in the other works quoted here is accurate when this coupling is described by Hund's Case (a) coupling and satellite bands are not present. In many of the transitions treated here, the coupling is somewhere between Hund's cases (a) and (b). In this case, the approach of Hill and Van-Vleck¹⁹ can be taken. The orbital angular momentum can also result in doublet peaks (Λ -doubling), but this effect is typically small relative to our experimental resolution, and has been neglected here.

To determine the vibrational temperature (T_{vib}), the integrated band intensity ($I_{\nu\nu'}$) is fit according to:

$$I_{\nu\nu'} \propto \nu^4 S_{\nu\nu'} \exp(-E_{\nu} / kT_{\text{vib}})$$

where E_{ν} is the energy of the excited state, ν is the frequency of light emitted, k is Boltzmann's constant and $S_{\nu\nu'}$ is the band strength for that transition. The band origin is used as the frequency and the other values are obtained from literature. Often, the Franck-Condon factor can be used instead of the band strength, as relative values of the

band strength typically agree with them to within a few percent. We use the Franck-Condon factors when the band strengths are not available.

The details of fitting vary slightly for each species, and will be given below.

A. CF ($B^2\Delta-X^2\Pi$)

CF shows two distinct peaks in the ultraviolet, due primarily to the (0,0) and (0,1) vibrational transitions of the $B^2\Delta-X^2\Pi$ electronic transition. These transitions were measured and fit by Carroll and Grennan²⁰ using the theory of Hill and Van Vleck. It should be noted that their constants do not accurately fit their values reported for the Q_2 branch at higher values of J ($J = 24.5-35.5$). However, if these peaks are instead assigned to the $^PQ_{12}$ branch ($J = 11.5-22.5$), the fit remains accurate. We have assumed that these peaks were incorrectly assigned, therefore their rotational constants are valid. The (0,0) band at 203 nm has an unresolved overlap with the (1,1) and (2,2) vibrational bands. A fit to the (0,0) band alone thus yields a poor fit of the spectrum. The (1,1) band has not been measured directly, however Carroll and Grennan do have rotational constant estimates for $v' = 1$ and $v'' = 1$ from the (1,2) and (0,1) bands, respectively. The (1,1) band origin is deduced from the reported $\Delta G(1/2)$ and $\Delta G(3/2)$. The (2,2) transition is approximated by linear extrapolation of the band origin and upper state rotational constants and the (0,2) transition data is used for the lower state constants. The (0,1) band at 208 nm is overlapped by the (1,2) and (2,3) bands. The (1,2) band was measured by Carroll and Grennan, however they did not report a value for the rotational constant A'' . This value was, however, determined in their (0,2) fit, and is critical to correctly fitting the spectrum. The rotational constants for the (2,3) band is estimated by linear

extrapolation of the (0,1) and (1,2) band values. We are able to estimate the band origin of the (2,3) band at $47,811\text{ cm}^{-1}$ from its three identifiable peaks. To determine the vibrational temperature, the Franck-Condon factors of Wentink and Isaacson are used.²¹

B. C_2 ($d^3\Pi_g - a^3\Pi_u$)

The C_2 swan bands, easily observed near 520 nm, are attributable to the excited triplet states of C_2 . The energy levels calculated in this work is based on the Hamiltonian and measured constants of Prasad and Bernath.²² An approach analogous to that of Hill and Van Vleck¹⁹ is used to calculate the intensities of transition. Because the Hamiltonian used is derived from a Hund's case (a) basis set, the case (a) intensity formulas can be multiplied by the appropriate orthonormal eigenvectors from the Hamiltonian solution to yield intensities for all transitions, including satellite bands. The (0,0) band is most prominent, though it is overlapped by the (1,1) band and the CO Angstrom system (0,2) band. All three bands are fit simultaneously. The tail of the (1,1) band is overlapped by the (2,2) band and an unidentified continuum. The unidentified continuum perturbs the fit significantly, so this part of the spectrum is omitted from the fit. The (0,1) Swan band is fit simultaneously with the (1,2) and (2,3) Swan bands and the (0,3) band of CO. The band strengths reported by Danylewych and Nicholls are used to estimate the vibrational temperature in both band systems.²³

C. CO (Angstrom and 3rd Positive Bands)

CO has two observed bands, the Angstrom system in the visible and the 3rd positive bands in the UV. The Angstrom band is due to the $B^1\Sigma - A^1\Pi$ electronic transition. The (0,2) and (0,3) transitions at 520 and 560 nm overlap with the C_2 Swan bands, while the (0,1) band can be identified independently. The (0,1) and (0,2) bands

are fit using the rotational constants of Kepa and Rytel.²⁴ Kepa and Rytel do note that there is some rotational perturbation in these states, which is not accounted for in this analysis. The (0,3) band was not included in their analysis, so constants reported by Krupenie are used instead.²⁵ Both the (0,2) and (0,3) bands must be fit simultaneously with the (0,0) and (0,1) Swan bands of C₂, respectively. The (0,0) Angstrom band is observable, but is within the noise of the spectrometer, and thus accurate fits cannot be performed. The 3rd Positive CO bands fall in the range of 280-330 nm and are due to the transition from triplet states $b^3\Sigma^+ - a^3\Pi$. The approach used to fit these bands is the same as that used for the C₂ Swan bands. The fitting constants used are those tabulated by Krupenie.²⁵ Vibrational temperatures are not obtained for these bands because the bands originating from the higher vibrational modes are too weak to make an accurate intensity estimate.

D. SiF ($A^2\Sigma - X^2\Pi$)

SiF gives prominent peaks from 430-450 nm. The nature of this transition is similar to that of the CF transition, except that ΔA is of opposite sign. Johns and Barrow measured the constants for the (0,0) transition.²⁶ However, they did not report any constants for the overlapping (1,1) and (2,2) bands. For this reason, only their measured (0,0) band origin is used, and the remaining constants for these three bands are drawn from the same sources for consistency. The lower state constants are taken from the C-X study of Appelblad, et. al.²⁷ and the upper state constants are taken from a study of the C-A electronic transition fit by Houbrechts, et. al.²⁸ The higher wavelength portion of the (2,2) band is not included in the fit, as it is overlapped by the (3,3) band, for which the

ground state constants were not measured. The Franck-Condon factors measured by Wentink and Spindler are used to extract a vibrational temperature.²⁹ Some second order diffraction lines from atomic Si overlap these spectra. The intensity of each of these lines is also fit with the spectrum so that they do not perturb the fit values.

E. CN ($B^2\Sigma^+-X^2\Sigma^+$)

CN is present due to interaction of carbon species with trace amounts of nitrogen in the chamber, and gives a readily identified band due to the $B^2\Sigma^+-X^2\Sigma^+$ transition near 380 nm. The analysis of Prasad, et. al. of this electronic transition is used to determine the energy levels of the spectrum.³⁰ They classified both states as Hund's case-(b), so the appropriate intensity factors for case-b doublets is used in calculating the intensities.³¹ The most prominent band is due to the (0,0) vibrational transition, and is overlapped by transitions described by (v,v). In this work values of v from 0 to 5 are used to fit the spectrum, based on the availability of bandstrength measurements.³² A 2nd order diffraction line attributable to atomic carbon overlaps this spectrum, and is fit simultaneously. While higher order vibrational bands will overlap this part of the spectrum, their intensities will be relatively small. This spectrum is not fit below 382 nm to prevent an overlapping continuum emission from interfering with the fit.

IV. Results

The resulting fit spectra are shown in Figures 1-5. The spectra were fit in two different fashions. First, the spectra were fit assuming the same rotational temperature for all vibrational modes and fitting independently the vibrational temperature, rotational temperature and intensities. These results are summarized in Table I. The fits were also

attempted allowing each vibrational band to have a different rotational temperature. These fits are those represented in the figures, and are summarized in Table II. Individual fit results will be discussed on a molecule-by-molecule basis.

A. CF ($B^2\Delta-X^2\Pi$)

The CF bands due to the (0,0) and (0,1) transitions and their fits are shown in Figure 1. If the (0,0) band is fit without including the overlapping (1,1) and (2,2) bands, $T_{rot} \sim 1980$ K is obtained, and the fit is fairly poor. When the (1,1) and (2,2) bands are included, with intensities determined by the Frank-Condon factors and a fit vibrational temperature, the band yields a rotational temperature of 1345 K and a vibrational temperature of 2731 K. When the rotational temperatures are allowed to vary independently for the different bands, a rotational temperature of 1247 K is obtained for the (0,0) band and 2338 K for the (1,1) and (2,2) bands. The vibrational temperature is 5948 K. For the (0,1) band it is necessary to include all of the (0,1), (1,2) and (2,3) bands to get a reasonable fit. When fit together, the rotational temperature is 2806 K with a vibrational temperature of 2486 K. Allowing different rotational temperatures gives 1209 K for the (0,1) band and 3049 K for the higher order bands. The vibrational temperature here is 5630 K. These high vibrational and rotational temperatures for the upper vibrational states result from fitting the tail end of the band. If more higher order bands were included, a more reasonable fit of these higher order states is expected.

B. C_2 ($d^3\Pi_g-a^3\Pi_u$)

The C_2 fit, shown in Figure 2, yields a rotational temperature of 1845 K and 2016 K for the two different band systems when the states are assumed to have the same

rotational temperature. The simultaneous CO fit yields a T of 630 K and 1273 K. The integrated band strength for C₂ gives a ratio of 0.254 for the (1,1) to (0,0) transitions, giving an estimated vibrational temperature of 4434 K. The best fit of the (0,1), (1,2) and (2,3) intensities gives a vibrational temperature of 3174 K. If the rotational temperature of each transition is fit separately, we find 1890 K for the (0,0) transition and 1756 K for the (0,1) transition. The higher order transitions show greater variations with temperatures of 1433 K and 3653 K. Vibrational temperatures of 3421 and 9352 K are obtained for these two bands. In fitting, the tail of the (1,1) transition is omitted because it is overlapped by an unidentified continuum that interferes with the fit. This may be responsible for the lower fit temperature in the (1,1) transition. The fit of the (0,1), (1,2) and (2,3) band are also heavily affected by instrument noise levels.

C. CO (Angstrom and 3rd Positive Bands)

The CO Angstrom bands are included in Figure 2 and the 3rd positive bands in Figure 3. The (0,2) and (0,3) Angstrom bands were fit simultaneously with the C₂ Swan Bands, as discussed above, while the (0,1) band is fit alone. The (0,1) band is not well distinguished from detector noise, so the fit is not shown in Figure 2. These three bands give rotational temperatures of 1220 K, 630 K and 1273 K, respectively. The (0,3) band temperature shifts 100 K lower when the method for fitting the C₂ bands is changed. The 3rd positive bands do not overlap and are therefore each fit independently, hence the identical values in Tables I and II. These bands give rotational temperatures of 1540 K, 1689 K and 1145 K. This disagreement in fits might suggest some large error bars in the fit, as the bands all originate out of the same state. For the 3rd positive system, the integrated intensities, after the v^4 correction, are in the ratio 0.69:1.00:0.50, compared to

Krupenie's band strength ratios of 0.66:1.00:0.80.²⁵ This indicates the (0,2) band fit is weaker than it should be, and its fit value is likely not as good as the other two bands due to the level of noise and baseline fluctuation in the measurement.

D. SiF ($A^2\Sigma-X^2\Pi$)

The SiF bands are depicted in Figure 4. The fit yields a rotational temperature of 2186 K and vibrational temperature of 2165 K when only one rotational temperature is assumed for the entire system, suggesting the rotational and vibrational temperatures may be equilibrated. However, when multiple band temperatures are used, the rotational temperatures range from 930 to 2448 K, and the vibrational temperature is lower at 1746 K. The fit fails to capture the spectrum well near the (0,0) band origin (437 nm). This may indicate that the rotational distribution is not fully equilibrated.

E. CN ($B^2\Sigma^+-X^2\Sigma^+$)

The CN band fit is shown in Figure 5. When only one rotational temperature is used, a rotational temperature of 1295 K and vibrational temperature of 5976 K are obtained. The effect of neglecting the higher order vibrational transitions was also examined. Bandstrengths for the (6,6) and (7,7) bands were estimated by extrapolating the reported strengths for the (v,v) series.³² The extrapolation function used was that of an exponential decay to a constant value. The vibrational temperature decreased to 5819 K when these extra bands were added in, even though their peak intensities are more than two orders of magnitude less than the first two bands. If the vibrational temperature is examined versus the number of bands included, it is seen to exponentially approach a value of 4818 K, so may be overestimated by as much as 1000 K.

V. Discussion

The results reported here yield fit rotational temperatures varying from anywhere between 630 K to as much as 3049 K and vibrational temperatures ranging from 1746 K to 9352 K. However, many of these discrepancies can be explained in terms of approximations or errors in the fitting procedure. In the case of CF, the tail end of the band is overlapped by higher vibrational modes, whose fitting constants are unknown. Because of this lack of fundamental information, it is not possible to properly include these modes, resulting in an artificially high rotational temperature for the higher order bands that are included in the fit. This will also have the effect of increasing the estimated vibrational temperature for CF. For C₂, CN and SiF, it was necessary to exclude the tail of the band because of uncharacterized overlapping spectra. Excluding these also affect the fits, likely reducing the band temperature of the higher order spectra. In the case of C₂ and SiF, it may also reduce the vibrational temperature. For CN, the vibrational temperature is overestimated because of insufficient data on higher vibrational modes. The CO bands are at fairly low intensities and are adversely affected by noise. The fits of the Angstrom bands only roughly captures the spectrum, and two of them are overlapped by the C₂ bands. The temperatures fit for the Angstrom bands are therefore dependent on the quality of the C₂ fit. The 3rd positive (0,0) and (0,1) bands give roughly similar temperatures, while the 3rd positive (0,2) band differs significantly from these two. As discussed earlier, the intensity fit by the (0,2) band is not consistent with the published band strengths of CO, making its fit suspect.

When these suspect fits are discarded, there is still variation in fit temperatures between the different species. The CF bands yield consistent temperature based on their $v' = 0$ fits, and the rotational temperature from CF is estimated at 1230 ± 30 K. The

rotational temperature of the CN radical is found to be consistent with this based on its first two bands, and can be estimated as 1260 ± 60 K. CF and CN also have similar vibrational temperature estimates, near 5800 K. Other species yield higher rotational temperatures, however. The rotational temperatures of CO and C₂ could be estimated at 1615 ± 105 K and 1823 ± 95 K, respectively, while the SiF rotational temperature is 2290 ± 220 K. These error bars may seem large on initial inspection, but if one considers that they represent an uncertainty of <10%, they do not seem so unreasonable. Some of these errors and mean values are estimated assuming that the different vibrational modes have identical rotational temperatures, which is not necessarily true, however the fact that they agree to within 10% may indicate this is a reasonable assumption. It may be possible that SiF is, in fact, not equilibrated at all, as evidenced by the poor fit near the band origin.

There is some question as to the proper way to assign the Boltzmann population of states. In some works, the energy levels of the upper state have been used,^{4,5} while others have assumed the molecule to be populated according to the energy distribution of the ground state.^{6,7,15} If the state is long-lived enough to undergo many collisions before it decays via emission, its rotational states will equilibrate and the upper state energy distribution can be used. This is rarely the case, however, especially at low pressures. If this is not the case, the equilibration of the upper state depends on the means of excitation. It is probable the state will be created by electron impact. In this case, it is commonly argued that electron impact excitation cannot change the rotational angular momentum, so that the rotational distribution of the emitting state must be the same as that of the ground state. However, there are other assumptions involved. Electron impact could change the vibrational mode of the molecule, or, for free radicals, the spin state,

both of which will affect how the rotational distribution is populated in the excited molecule. The excited state could be produced from a multiple step collision process, i.e. by decay from a higher state or through excitation of a lower energy excited state. Or, the excited molecule may be a product of reaction from another species (i.e. chemiluminescence). Any collisions occurring within the time frame it takes for the excited state to decay will cause the rotational distribution to approach the excited states' equilibrium. If all of these effects are considered negligibly small, then the rotational distribution of the ground state is the appropriate distribution.

Realistically, the molecule is likely to fall into some intermediate regime, where it is not populated according to the ground state or upper state energies, but rather is somewhere between the two. The error induced by choosing the wrong state can be roughly estimated by considering the ratio of each state's rotational constants, B . To a first approximation, the intensity dependence on the population distribution comes from:

$$I \propto \exp(-hcE/kT_{rot}) \sim \exp(-hcBJ(J+1)/kT_{rot})$$

And therefore any error in the value of B used will be approximately proportional to the error in T_{rot} resulting from this approximation. For CF, SiF and CN in this work, the fit is based on the rotational constants of the ground state. The two B values for SiF agree to within one percent, so a temperature fit with the upper, rather than lower, state should agree to within one percent for SiF. For CF, the ground state constants are larger by 7%, respectively so the temperature determined by using the upper state constants would be 7% lower. For CN, the upper state constants are 4% higher, and the temperature fit would be 4% higher. For C_2 , the upper state constants were used. This constant is about 7% larger than the ground state. Therefore, using the ground state constant would give a

temperature near 1700 K, rather than 1820 K. The CO lines were based on the upper state, whose rotational constants for 3rd positive and Angstrom bands are both less than 2% larger than the ground state, meaning the temperatures may be overestimated by 30 K or less.

Even considering these potential sources of error, the data still suggests different rotational temperatures in different plasma species. There are a few reasons why this might be the case. One possibility is that the species are not equilibrated with each other. Another possibility is that the different temperatures are due to spatial variation in concentration and temperature. Neither the temperature nor concentration are guaranteed to be uniform in the plasma; indeed simulations predict that they are not.¹ As the emission measurements are not spatially resolved, the temperature of each species will be best characterized by the region where its density is greatest. In considering the five species examined here, they can be divided into three temperature ranges: CF and CN are at the lowest temperature, near 1250 K, C₂ and CO are next, between 1600-1800 K, and finally SiF, at 2300 K. The species CF and CN are likely produced by gas phase reactions, and may represent the temperature in the plasma bulk. Though evidence exists for surface production of CF in a capacitively coupled CF₄ plasma³³, or high density C₄F₈ plasmas,³⁴ surface production was not apparent for a continuously powered high-density CF₄ plasma.³⁵ Recent measurements show that C₂ can be produced by ion bombardment of surfaces in high density discharges,³⁶ and CO will be produced by etching of the quartz window. It is also possible for these species to be produced through gas phase interactions of the precursor gas and trace amounts of oxygen in the reactor. SiF, however, can only be produced from etching of the quartz window, whether it is

produced directly or by dissociation of other etch products. It appears that higher temperatures are associated with species that are produced from surfaces. This may indicate that the etch products leave the surface with significant energies, accounting for the higher temperatures of these species. It should be noted, however, that this trend is not consistent with measurements made in capacitive plasmas,⁷ although there are significant differences in neutral heating between inductive and capacitive plasmas, as evidenced by the magnitude of the temperature. A spatial temperature dependence of this nature is, however, consistent with Kiehlbach and Graves' model, where significant ion/neutral heating occurs in the sheaths.¹⁴ It is also noteworthy that the species with higher rotational temperatures have lower vibrational temperatures. This would suggest that the different species have undergone different degrees of equilibration between the rotational and vibrational modes. If this is true, it seems probable that the translational temperature is not fully equilibrated with the rotational or vibrational temperature.

The magnitudes of these temperatures (except SiF) show good agreement with those reported in Cl₂ plasmas by analysis of N₂ bands if their trends in pressure and power are extrapolated out to match these conditions.¹⁵ These temperatures are also nearly consistent with linewidth measurements in inductively coupled Ar plasmas.⁹ The numbers, however, significantly exceed those reported in our model of this system.¹ This is because the model did not include the significant heating mechanisms suggested in these other works. In Cl₂, heating was attributed to energy gained on dissociation of the parent Cl₂ gas. While the dissociation of molecules is generally an endothermic process, energy will be gained due to Franck-Condon heating. This was neglected in our model of CF₄ because it has not been well characterized. Using approximated values for this

process, Kiehlbach and Graves found this to be one of the major heating mechanisms.¹⁴ In the Ar plasma, where there is no dissociation processes, ion heating in the presheath and subsequent charge exchange play important roles in determining temperature. Ion heating was not treated in our model. Another mechanism that was not treated in our model, but was attributed to 10% of heating by Kiehlbach and Graves, is gas heating by vibrational-translational relaxation. The modeling code does not treat non-equilibrium between rotational and vibrational states, and therefore this heating mechanism is neglected.

VI. Conclusions

In this work, we have examined the approach of extracting rotational temperature from an inductively coupled CF₄ plasma. In doing so, assumptions regarding temperature equilibration amongst different species is also addressed. It is found that, at pressures of 30 mtorr and power densities near 0.7 W/cm³, reliable fits of the rotational spectrum vary from 1200-2300 K depending on the species used. Vibrational temperatures vary from 1700-5700 K. The species CF and CN, which are believed to be produced in the plasma, yield rotational temperatures near 1250 K, while C₂ and CO, which are produced both in the plasma and by plasma-surface interactions yield higher temperatures near 1600 K. SiF, an etch product from the quartz coupling window is at a rotational temperature near 2300 K. These results indicate a few different possible phenomena. One possible reason is that the species temperature depends on the means by which it is produced. It appears that species created at the chamber surfaces, likely by ion bombardment, possess higher

rotational energies. This may also indicate spatial variation in the temperature, with the temperature being elevated near the reactor surfaces. Finally, it is possible that equilibration of the rotational distribution with itself and the translational temperature is not fully achieved. In the case of SiF, the rotational envelope is not accurately fit by the equilibrated model. Comparing trends in rotational and vibrational temperature, it appears that the two modes are at various degrees of equilibration. A more detailed study of this technique, i.e. comparison to Doppler linewidth measurements, should be carried out to confirm the accuracy of this technique.

Acknowledgements

The authors would like to acknowledge the technical assistance of Jeff Ifland and Anthony Lombardi. We would also like to thank David Hash for useful discussion. The work of Dr. Rao and Dr. Cruden is funded by NASA-ARC contract to Eloret.

References

- ¹ D. B. Hash, D. Bose, M. V. V. S. Rao, B. A. Cruden, M. Meyyappan, and S. P. Sharma, *J Appl Phys* **90**, 2148-2157 (2001).
- ² T. A. Cleland and D. W. Hess, *J Appl Phys* **64**, 1068-1077 (1988).
- ³ M. Haverlag, F. J. de Hoog, and G. M. W. Kroesen, *J Vac Sci Techn A* **9**, 327-330 (1991).
- ⁴ M. Oshima, *Jpn J Appl Phys* **17**, 1157-1158 (1978).
- ⁵ A. Chelouah, E. Marode, G. Hartmann, and S. Achat, *J Phys D: Appl Phys* **27**, 940-945 (1994).
- ⁶ R. A. Porter and W. R. Harshbarger, *J Electrochem Soc*, 460-464 (1979).
- ⁷ G. P. Davis and R. A. Gottscho, *J Appl Phys* **54**, 3080-3086 (1983).
- ⁸ M. Haverlag, E. Stoffels, W. W. Stoffels, G. M. W. Kroesen, and F. de Hoog, *J Vac Sci Techn A* **14**, 380-3 (1996).
- ⁹ G. A. Hebner, *J Appl Phys* **80**, 2624-2636 (1996).
- ¹⁰ T. Nakano, N. Sadeghi, and R. A. Gottscho, *Appl Phys Lett* **58**, 458-460 (1991).
- ¹¹ V. M. Donnelly, *J Appl Phys* **79**, 9353-9360 (1996).
- ¹² H. Singh, J. W. Coburn, and D. B. Graves, *J Vac Sci Technol A* **19**, 718-729 (2001).
- ¹³ B. A. Cruden, M. V. V. S. Rao, S. P. Sharma, and M. Meyyappan, *Plasma Sources Sci Technol*, submitted (2001).
- ¹⁴ M. W. Kiehlbauch and D. B. Graves, *J Appl Phys* **89**, 2047-2057 (2001).
- ¹⁵ V. M. Donnelly and M. V. Malyshev, *Appl Phys Lett* **77**, 2467-2469 (2000).

- ¹⁶ J. S. Kim, M. V. V. S. Rao, M. A. Cappelli, S. P. Sharma, and M. Meyyappan, *Plasma Sources Sci Technol* **10**, 191-204 (2001).
- ¹⁷ B. A. Cruden, M. V. V. S. Rao, S. P. Sharma, and M. Meyyappan, *J Vac Sci Techn B*, submitted (2001).
- ¹⁸ M. V. V. S. Rao, S. P. Sharma, B. A. Cruden, and M. Meyyappan, *Plasma Sources Sci Technol*, submitted (2001).
- ¹⁹ E. Hill and J. H. Van Vleck, *Phys Rev* **32**, 250-272 (1928).
- ²⁰ P. K. Carroll and P. K. Grennan, *J Phys B: Atom Molec Phys* **3**, 865-877 (1970).
- ²¹ T. Wentink, Jr. and L. Isaacson, *J Chem Phys* **46**, 603-605 (1967).
- ²² C. V. V. Prasad and P. F. Bernath, *Astrophys J* **426**, 812-821 (1994).
- ²³ L. L. Danylewych and R. W. Nicholls, *Proc R Soc Lond A* **339**, 197-212 (1974).
- ²⁴ R. Kepa and M. Rytel, *J Phys B: At Mol Opt Phys* **26**, 3355-3362 (1993).
- ²⁵ P. H. Krupenie, *The Band Spectrum of Carbon Monoxide*, Vol. 5 (National Bureau of Standards, Washington, DC, 1966).
- ²⁶ J. W. C. Johns and R. F. Barrow, *Proc Phys Soc A* **71**, 476-484 (1958).
- ²⁷ O. Appleblad, R. F. Barrow, and R. D. Verma, *J Phys B (Proc Phys Soc)* **1**, 274-282 (1968).
- ²⁸ Y. Houbrechts, I. Dubois, and H. Bredohl, *J Phys B: At Mol Phys* **15**, 603-611 (1982).
- ²⁹ T. Wentink, Jr. and R. J. Spindler, Jr., *J Quant Spectrosc Radiat Transfer* **10**, 609-619 (1970).
- ³⁰ C. V. V. Prasad, P. F. Bernath, C. Frum, and R. Engleman, Jr, *J Mol Spectrosc* **151**, 459-473 (1992).

- ³¹ W. Jevons, *Report on Band-Spectra of Diatomic Molecules* (The Physical Society, London, 1932).
- ³² L. L. Danylewych and R. W. Nicholls, *Proc R Soc Lond A* **360**, 557-573 (1978).
- ³³ J. P. Booth, G. Cunge, P. Chabert, and N. Sadeghi, *J Appl Phys* **85**, 3097-107 (1999).
- ³⁴ C. Suzuki, K. Sasaki, and K. Kadota, *Jpn J Appl Phys I* **37**, 5763-6 (1998).
- ³⁵ C. Suzuki, K. Sasaki, and K. Kadota, *J Appl Phys* **82**, 5321-6 (1997).
- ³⁶ C. Suzuki, K. Sasaki, and K. Kadota, *Jpn J Appl Phys* **38**, 6896-6901 (1999).

List of Figures

Figure 1. Experimentally measured (solid line) and model fit (dashed line) for CF emission bands. (a) The (0,0), (1,1) and (2,2) bands. (b) The (0,1), (1,2) and (2,3) bands.

Figure 2. Experimentally measured (solid line) and model fit (dashed line) for the C₂ Swan emission bands and CO Angstrom bands. (a) The peaks below 5130 Å are due primarily to the C₂ (1,1) transition, the peaks below 5165 Å are primarily from the C₂ (0,0) band, and the peaks at higher wavelengths are from the CO (0,2) Angstrom band. (b) The (0,1), (1,2) and (2,3) Swan bands have their heads at 5636, 5586 and 5541 Å, respectively. These are overlapped by the (0,3) Angstrom band of CO, with its head at 5610 Å. Emission at higher wavelengths may be due to F₂.

Figure 3. Experimentally measured (solid line) and model fit (dashed line) for the observed CO 3rd positive emission bands. Shown are the transitions given by the (a) (0,0), (b) (0,1) and (c) (0,2) bands.

Figure 4. Experimentally measured (solid line) and model fit (dashed line) for the SiF emission bands. Also overlapping are several 2nd order diffraction peaks from atomic silicon. The bands and peaks are all labeled on the figure.

Figure 5. Experimentally measured (solid line) and model fit (dashed line) for the CN emission bands. Also overlapping is a 2nd order diffraction peak from atomic carbon. The first three bands and peak are labeled on the figure. Peaks due to transitions (v,v), v > 2, also fall in this region but are not easily distinguished.

Table I. Rotational and Vibrational Fit temperatures for different bands, with rotational temperatures assumed equal between different states.

Molecular Species (Transition)	Rotational Temp (K)	Vibrational Temp (K)
CF ($B^2\Delta-X^2\Pi$); $v' = v''$	1345	2731
CF ($B^2\Delta-X^2\Pi$); $v' = v''-1$	2806	2486
C ₂ ($d^3\Pi_g-a^3\Pi_u$); $v' = v''$	1845	4434
C ₂ ($d^3\Pi_g-a^3\Pi_u$); $v' = v''-1$	2016	3174
CO ($B^2\Sigma-A^1\Pi$)	1229 (0,1) 627 (0,2) 1273 (0,3)	N/A
CO ($b^3\Sigma^+-a^3\Pi$)	1540 (0,0) 1689 (0,1) 1145 (0,2)	N/A
SiF ($A^2\Sigma-X^2\Pi$)	2186	2165
CN ($B^2\Sigma^+-X^2\Sigma^+$)	1295	5976

Table II. Rotational and Vibrational temperatures fit for different emission bands. In this data, rotational temperatures are fit separately for each transition, except where two or more vibrational transitions are listed together.

Molecular Species (Transition)	Rotational Temp (K) (v', v'')	Vibrational Temp (K)
CF ($B^2\Delta-X^2\Pi$); $v' = v''$	1247 (0,0) 2338 (1,1)/(2,2)	5945
CF ($B^2\Delta-X^2\Pi$); $v' = v''-1$	1209 (0,1) 3049 (1,2)/(2,3)	5630
C ₂ ($d^3\Pi_g-a^3\Pi_u$)	1890 (0,0) 1433 (1,1)	3421
C ₂ ($d^3\Pi_g-a^3\Pi_u$)	1756 (0,1) 3653 (1,2)/(2,3)	9352
CO ($B^1\Sigma-A^1\Pi$)	1229 (0,1) 627 (0,2) 1173 (0,3)	N/A
CO ($b^3\Sigma^+-a^3\Pi$)	1540 (0,0) 1689 (0,1) 1145 (0,2)	N/A
SiF ($A^2\Sigma-X^2\Pi$)	2448 (0,0) 2139 (1,1) 930 (2,2)	1746
CN ($B^2\Sigma^+-X^2\Sigma^+$)	1220 (0,0) 1301 (1,1) 1570 (2,2) 1085 (3,3)/(4,4)/(5,5)	5761

Figure 1

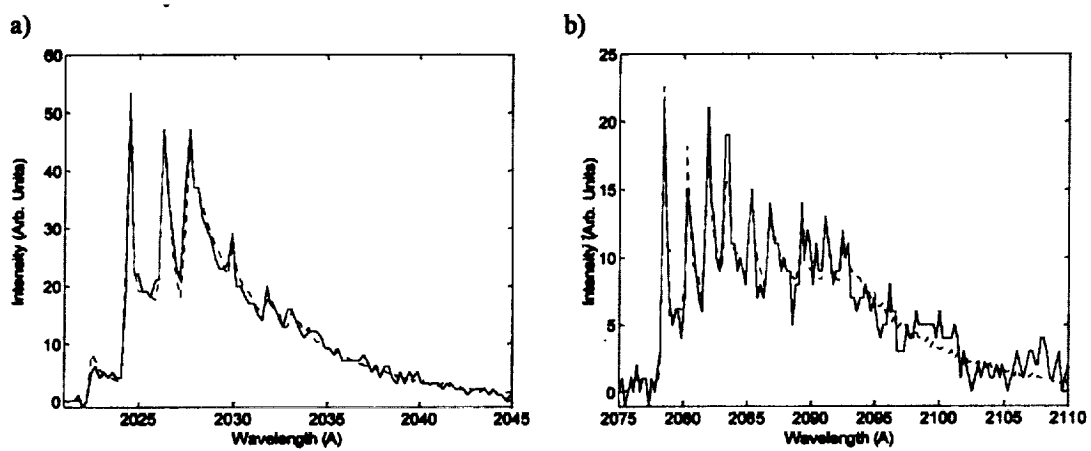


Figure 2

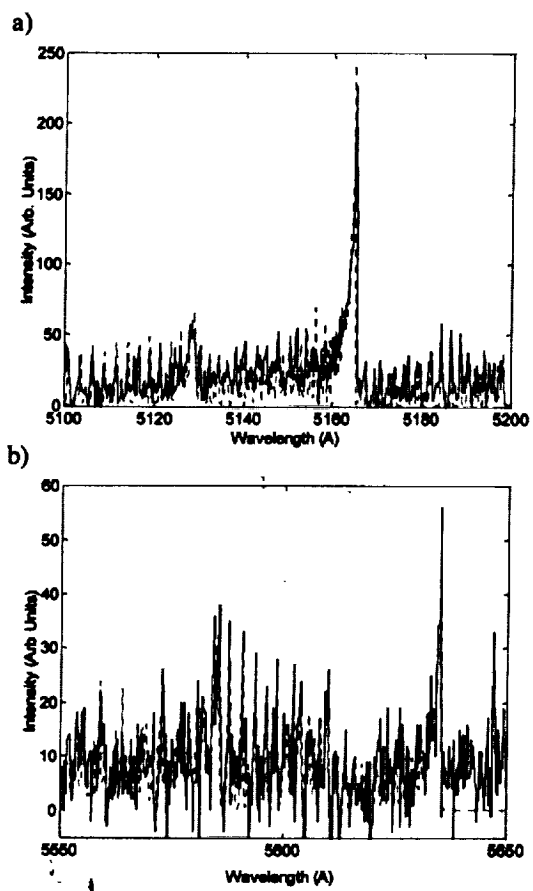


Figure 3

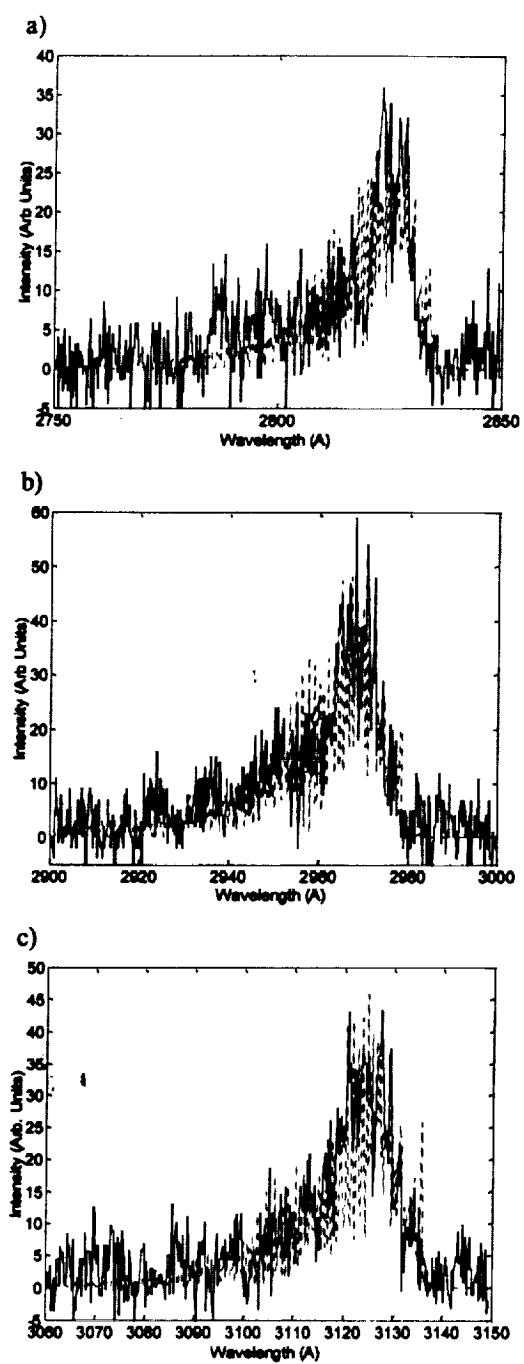


Figure 4

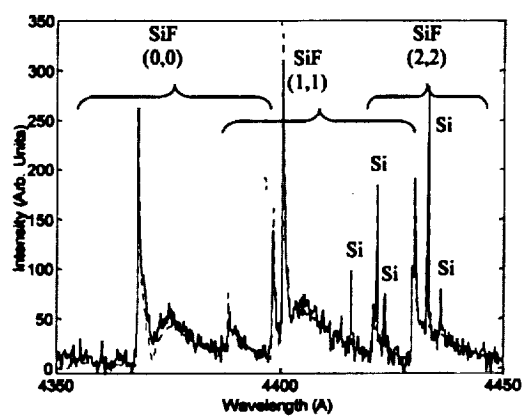


Figure 5

